Stanford Exploration Project, Report 110, September 18, 2001, pages 1–113

Short Note

Ray-based tomography with limited picking

Robert G. Clapp[1]

INTRODUCTION

In ray-based reflection tomography picking reflectors is an integral and painful part of the process (Clapp, 2001; van Trier, 1990; Stork, 1992; Kosloff et al., 1996). The general methodology is to pick a series of reflectors from a migrated image. A set of rays are then calculated that reflect at the picked interfaces. A major problem is the human intensive nature of reflector picking, especially for 3-D data. Automatic pickers can help, but significant human quality control (QC) is still necessary. A high level of QCing is required because inaccurate reflector picks lead to inaccurate reflector dip estimates, which in turn leads to back projecting information to the wrong portion of the model space, seriously hampering the inversion.

In this paper I present a method to eliminate, or at least significantly reduce, the need for reflector picking. I calculate a dip field and coherency from a migrated image by first using the plane-wave estimator from Claerbout (1992) and later used by Bednar (1997). I next refine the dip estimate using the methodology described in Fomel (2000). I then automatically select back projection points based on dip coherency and semblance strength. The method is applied to a 2-D North Sea Dataset. The turn around time is reduced significantly and the overall image quality is equal to or better than conventional reflector picking approach.

THEORY

Figure 1 shows the typical flow for ray-based reflection tomography.

- First a set of reflectors are picked. Then residual moveout analysis is performed along the reflectors.
- This moveout is characterized by one or more parameters.
- The reflectors are also used as the basis for back projection points. The normal of the picked reflectors is used either for calculating the initial takeoff angle (if shooting up

[1]**email:** bob@sep.stanford.edu

from the reflector) or for ensuring Snell's law is obeyed at the reflector (if shooting down to the reflector).

- Finally, time errors are estimated for each ray pair (Stork, 1992).

Two of the largest potential sources of error in this estimation scheme are an inaccurate dip estimate (causing information to back projected into the wrong portion of model space) and inaccurate description of moveout. The first type of error is the result of a poor description of the reflectors, which may be the result of overuse of an auto-picker or too little or too much smoothing of reflector positions. Poor moveout description is often the result of extending reflectors into areas with low signal-noise ratio where moveout analysis gives unreliable information. Both problems can be attenuating with significant human QCing, but will increase turnaround time.

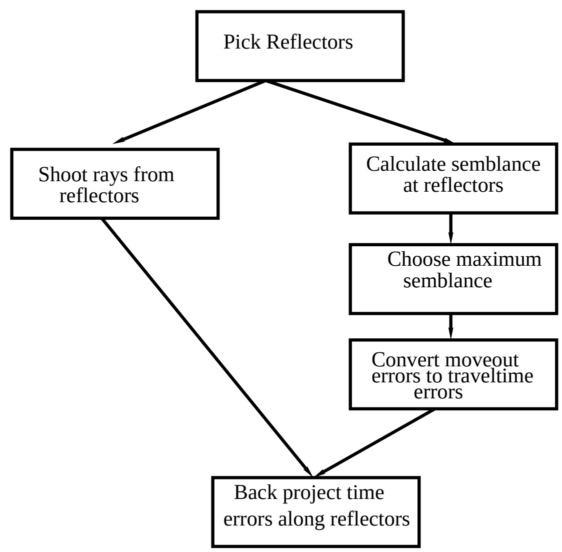

Figure 1: A typical ray-based reflection tomography loop. bob1-old [NR]

Figure 2 shows an alternate ray-based tomography flow. Rather than using picked reflectors as the basis for back projection locations, points are selected according to reliability factors. First dip and coherency of the migrated image is calculated at each image location. For an initial dip and coherence estimate I take a window around each model location. I calculate the best single dip within the region, and the coherence of that dip, using the method described in Claerbout (1992). I then use this as an initial dip estimate for the non-linear, space varying dip estimation procedure described in Fomel (2000).

Likely back projection points are then automatically selected by finding model locations that meet some specified dip coherence, amplitude, and distance from other selected points. To get the 'best' points in each region, these criteria are slowly relaxed (e.g. the first pass might look for points above the 90th percentile in amplitude and dip coherence, while the last pass might drop both these criteria to the 50th percentile.).

At each initially selected point semblance analysis is performed. Points that don't have good semblance (large semblance value and a definite maximum) are discarded. The remaining points are then used.

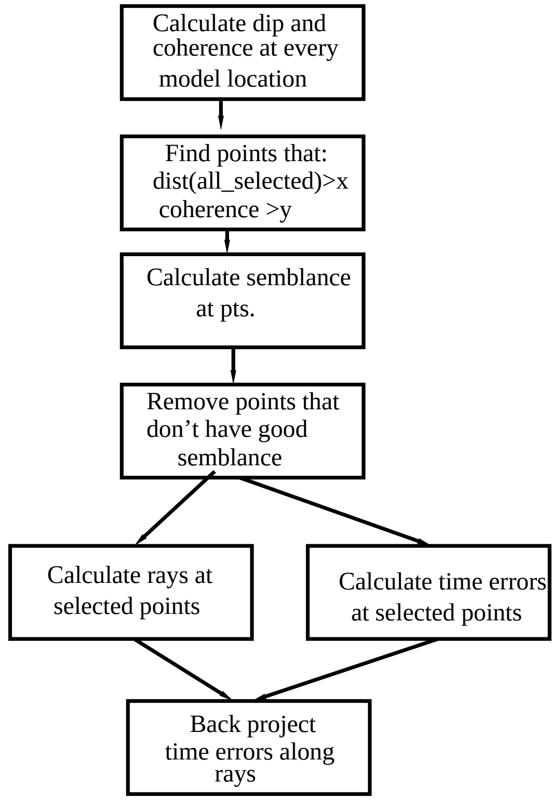

Figure 2: Back-projection scheme used in this paper. Note the absence of reflector picking. bob1-new [NR]

DATA EXAMPLE

To test the methodology I applied it on a 2-D North Sea line taken from a 3-D volume, the same dataset used in (Clapp, 2000, 2001). There is a significant 3-D component to the data, especially from the salt structure. Figure 3 shows the initial velocity model. The initial velocity model was created by smoothing to an extreme the S.M.A.R.T[2] method (Jacobs et al., 1992; Ehinger and Lailly, 1995). Figure 4 shows the initial migration (by doing split-step downward continuation) of the data and Figure 5 show every 10th CRP gather. Note how there is significant residual moveout throughout the model.

From this initial migrated image I calculated the dip (Figure 6) and coherence (Figure 7). To calculate the initial back projection points I selected points above 30th percentile in image amplitude, 45th percentile in dip coherence, and at least four model points away from all other selected points. I then calculated semblance at each point and parsed from the list points with semblance below .16 and whose maximum was less than 40% below the average semblance. Figure 8 shows the final location of back projection points. Note how there are few points near the salt body and in the lower portion of the image.

As image quality improves, the automatic selector slowly uses more and more model

[2]Sequential Migration-Aided Reflection Tomography - KIM (Kinematic Inversion Methods), IFP consortium

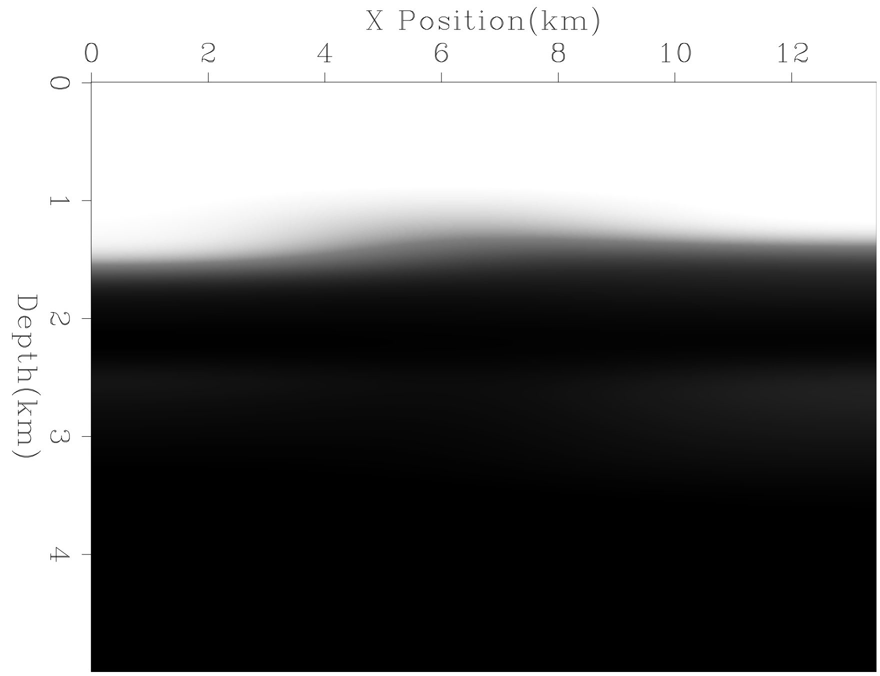

Figure 3: Initial velocity model. bob1-vel0 [CR]

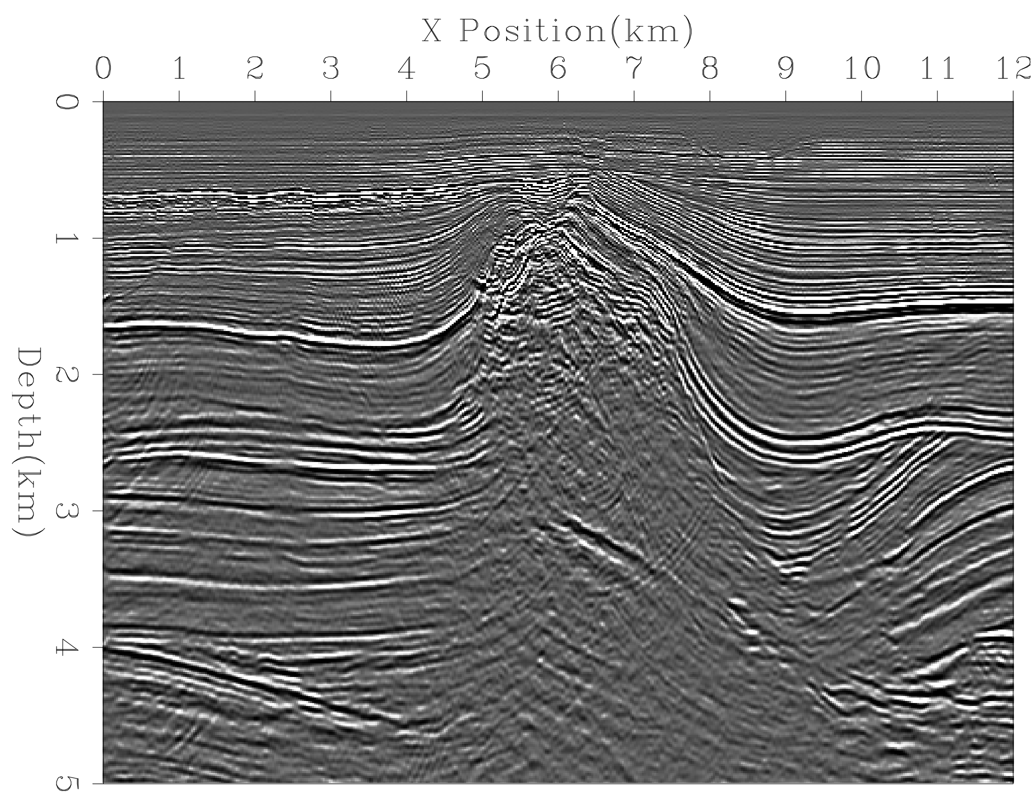

Figure 4: Initial migration using the velocity model shown in Figure 3. bob1-image.vel0 [CR]

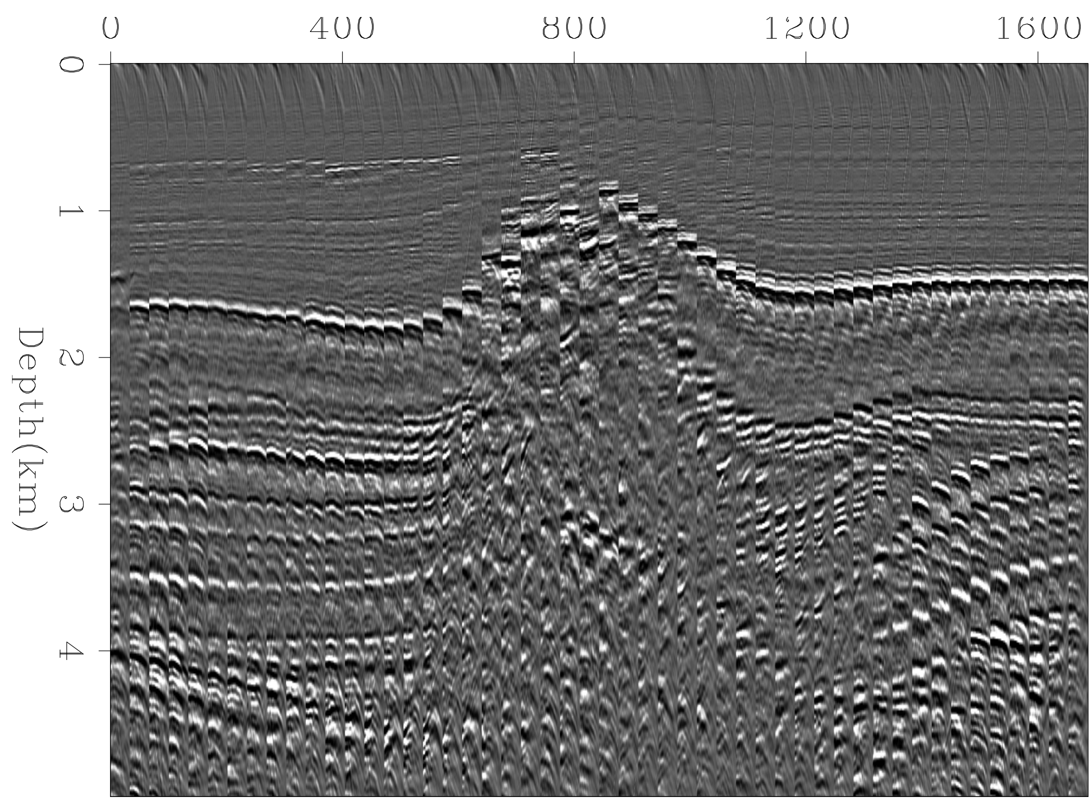

Figure 5: Every 10th CRP gather of the initial migration (Figure 4) using the velocity model shown in Figure 3. bob1-mig.vel0 [CR]

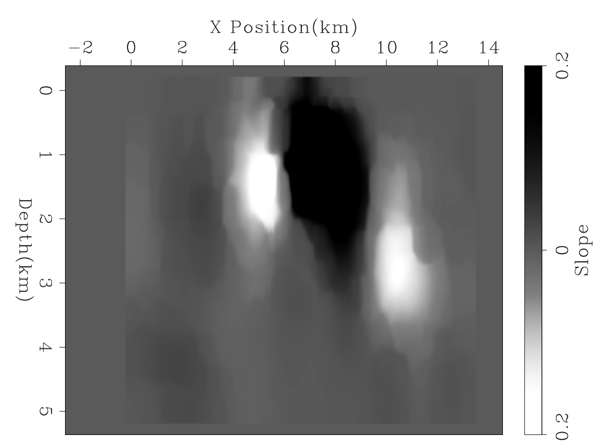

Figure 6: The calculated dip field for the initial migration image. bob1-dipxz.vel0 [CR]

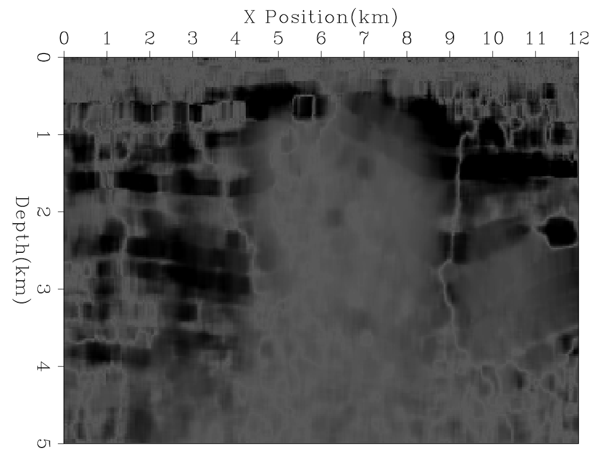

Figure 7: The calculated dip coherence for the initial migration image. bob1-coher.vel0 [CR]

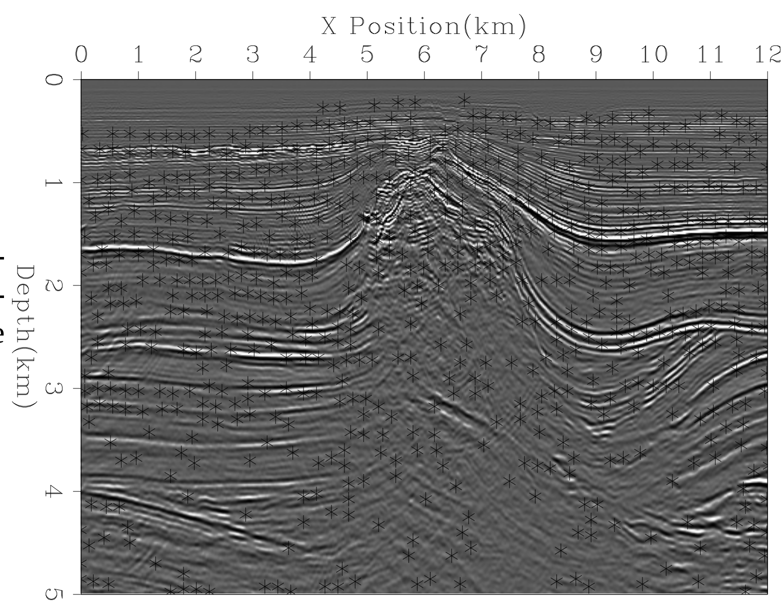

Figure 8: The selected back projection points. Note how the points generally follow reflectors and avoid the salt structure. bob1-pts.vel0 [CR]

points. Figure 9 shows the points selected after the five iteration of tomography. Note how there are now many more points in the lower portion of the model and closer to the salt. The velocity model after five iterations can be seen in Figure 10 and the resulting migrated image in Figure 11. Figure 12 shows the CRP gathers of the fifth migration. Note how they are significantly flatter than in Figure 12.

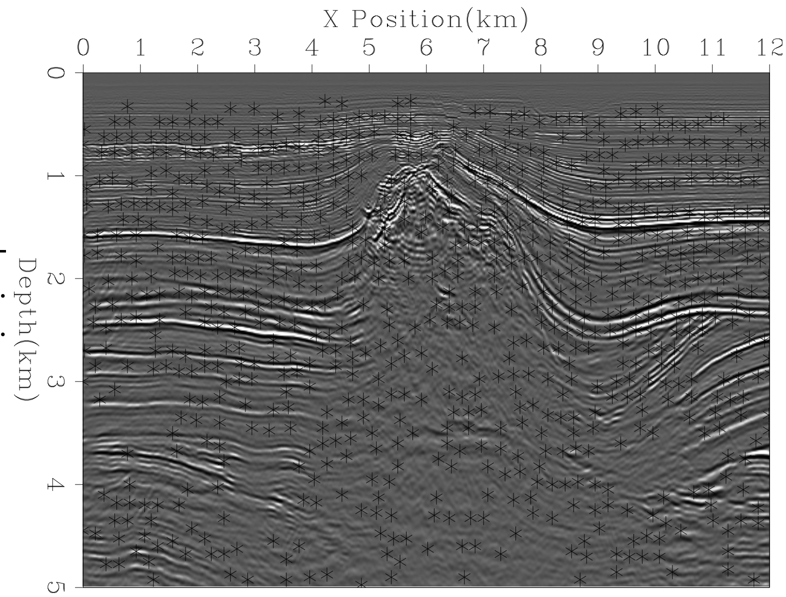

Figure 9: The selected back projection points after five iterations. Note the difference from Figure 8. bob1-pts.final [CR]

CONCLUSIONS

Reflector picking is one of the main bottlenecks in ray-based tomography. By automatically selecting back projection points based on dip coherency and high semblance, picking can be avoided. The results on a 2-D dataset are encouraging.

REFERENCES

Bednar, J. B., 1997, Least squares dip and coherency attributes: SEP–**95**, 219–225.

Claerbout, J. F., 1992, Earth Soundings Analysis: Processing versus Inversion: Blackwell Scientific Publications.

Clapp, R., 2000, Tau tomography with steering filters: 3-D field data example, preliminary result: SEP–**105**, 123–138.

Clapp, R. G., 2001, Geologically constrained migration velocity analysis: Ph.D. thesis, Stanford University.

Ehinger, A., and Lailly, P., 1995, Velocity model determination by the SMART method, part 1: Theory: 65th Annual Internat. Mtg., Soc. Expl. Geophys., Expanded Abstracts, 739–742.

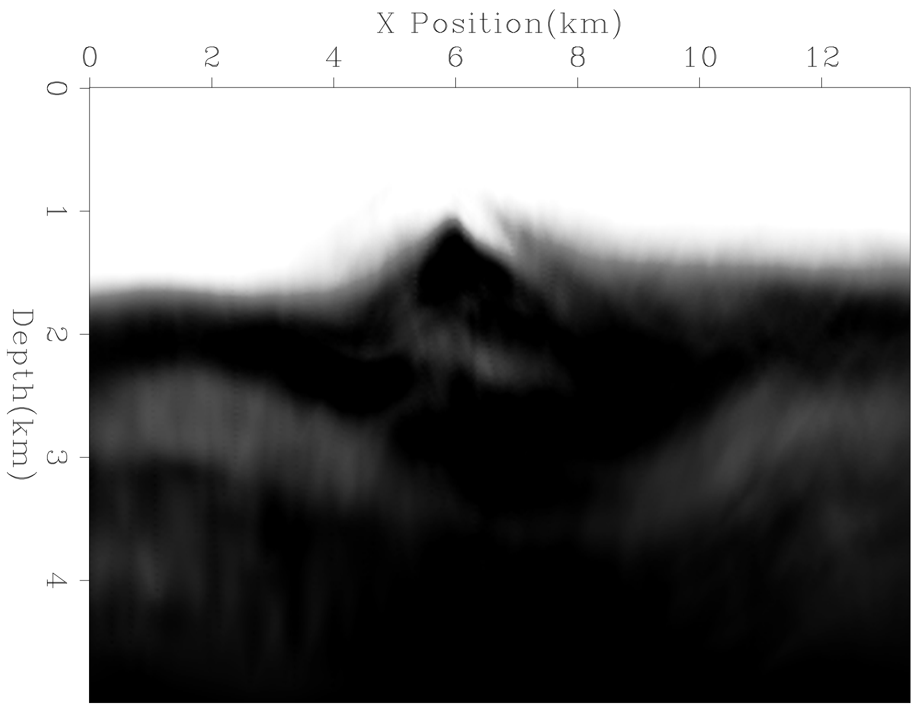

Figure 10: Final velocity model. bob1-final [CR]

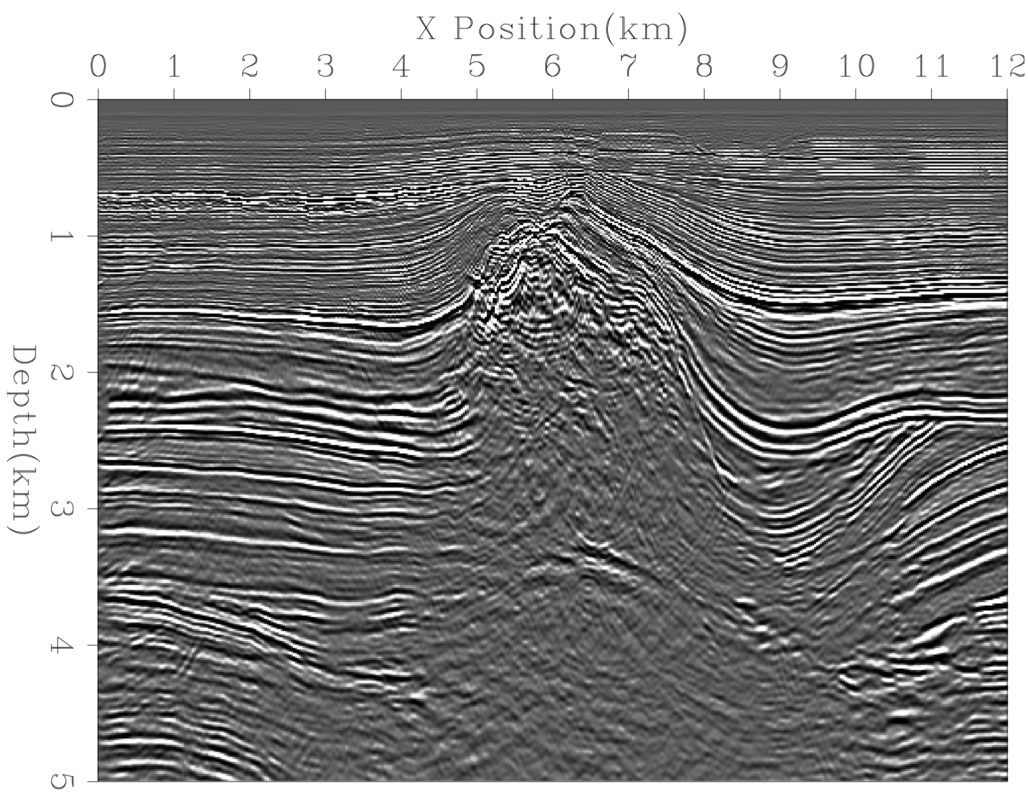

Figure 11: Final migration using the velocity model shown in Figure 10. bob1-image.final [CR]

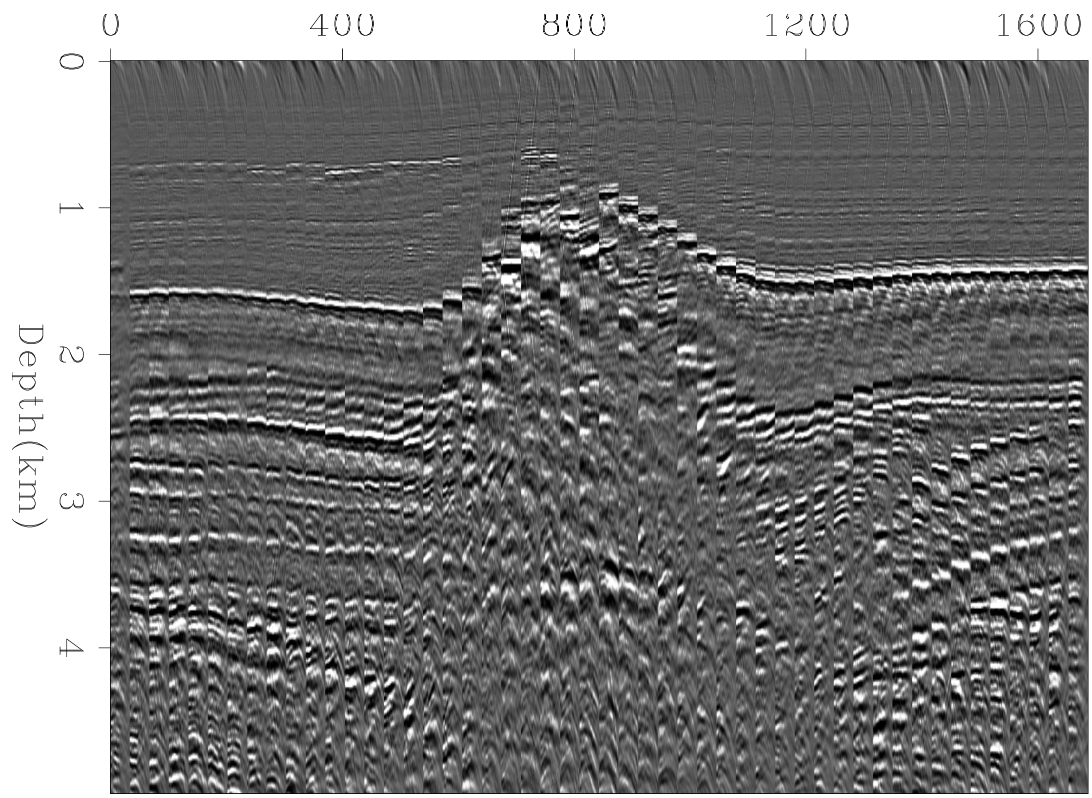

Figure 12: Every 10th CRP gather of the final migration (Figure 11) using the velocity model shown in Figure 10. bob1-mig.final [CR]

Fomel, S., 2000, Applications of plane-wave destructor filters: SEP–**105**, 1–26.

Jacobs, J. A. C., Delprat-Jannaud, F., Ehinger, A., and Lailly, P., 1992, Sequential migration-aided reflection tomography: A tool for imaging complex structures: 62nd Annual Internat. Mtg., Soc. Expl. Geophys., Expanded Abstracts, 1054–1057.

Kosloff, D., Sherwood, J., Koren, Z., MacHet, E., and Falkovitz, Y., 1996, Velocity and interface depth determination by tomography of depth migrated gathers: Geophysics, **61**, no. 5, 1511–1523.

Stork, C., 1992, Reflection tomography in the postmigrated domain: Geophysics, **57**, no. 5, 680–692.

van Trier, J., 1990, Tomographic determination of structural velocities from depth migrated seismic data: Ph.D. thesis, Stanford University.